Atomic diffusion behavior in Cu-Al explosive welding process

Liu, K. X.; Li, X. J.; Luo, N.; Lu, Guoxing.; Chen, S. Y.; Wu, Z. W.

2013

Chen, S. Y., Wu, Z. W., Liu, K. X., Li, X. J., Luo, N., & Lu, G. (2013). Atomic diffusion behavior in Cu-Al explosive welding process. Journal of Applied Physics, 113(4).

https://hdl.handle.net/10356/100640

https://doi.org/10.1063/1.4775788

Atomic diffusion behavior in Cu-Al explosive welding process

S. Y. Chen, Z. W. Wu, K. X. Liu, X. J. Li, N. Luo et al.

Citation: J. Appl. Phys. **113**, 044901 (2013); doi: 10.1063/1.4775788
View online: http://dx.doi.org/10.1063/1.4775788
View Table of Contents: http://jap.aip.org/resource/1/JAPIAU/v113/i4
Published by the American Institute of Physics.

Atomic diffusion behavior in Cu-Al explosive welding process

S. Y. Chen,[1] Z. W. Wu,[1] K. X. Liu,[1,2,a)] X. J. Li,[3] N. Luo,[1] and G. X. Lu[4]
[1]*LTCS and Department of Mechanics & Aerospace Engineering, College of Engineering, Peking University, Beijing 100871, China*
[2]*Center for Applied Physics and Technology, Peking University, Beijing 100871, China*
[3]*Department of Engineering Mechanics, Dalian University of Technology, Dalian 116024, China*
[4]*College of Engineering, Nanyang Technological University, 637457, Singapore*

(Received 12 November 2012; accepted 21 December 2012; published online 23 January 2013)

A hybrid method is proposed to study atomic diffusion behavior in Cu-Al explosive welding process. The method combines molecular dynamics simulation and classical diffusion theory. Cu-Al explosive welding and scanning electron microscope experiments are done to verify the method. Using the method, we find that the atomic diffusion mostly takes place in the unloading stage of the welding process. The diffusion coefficients are collision velocity-dependent, with higher velocities generating larger coefficients. When there is no transverse velocity, the diffusion coefficient is directly proportional to the longitudinal velocity. With the longitudinal velocity fixed, the diffusion coefficient is proportional to the square of the transverse velocity. The thickness of the diffusion layer is calculated from the simulation result, and it is in good agreement with the experiment result. © *2013 American Institute of Physics*. [http://dx.doi.org/10.1063/1.4775788]

I. INTRODUCTION

Explosive welding has been widely applied in industrial production for decades. It is well known for its capability to directly join a wide variety of both similar[1,2] and dissimilar[3–5] combinations of materials that can hardly be joined by any other welding techniques.[6] Since its inception, its physical process and mechanism have received extensive attention,[2,7,8] but they are still not completely clear. Diffusion, as one of the important physical phenomena which are accelerated by explosive treatment during the welding process, has a close relationship with the morphology of the bonding interface and the welding quality. Besides, the diffusion process and the diffusion layer thickness affect the mechanical properties and electromagnetic properties of the weldment directly or indirectly. In-depth studies for the atomic diffusion behavior have great significance for the practice of explosive welding engineering, and it will be an entry point for the studies of the improvement of explosive welding. Experimental studies on atomic diffusion in the explosive welding processes have been carried out. Akbari Mousavi and Sartangi[9] obtained the composition-penetration plots after the diffusion across the interface of the explosively welded cp-Titanium/AISI 304 stainless steel composites from energy dispersive spectroscopy (EDS) microanalysis. Hokamoto *et al.*[10] measured and analyzed elemental distribution after the diffusion across the interfacial zone for metallic glass and stainless steel. In contrast, simulations at atomic scale of atomic diffusion in the explosive welding processes have scarcely been done.

Molecular dynamics (MD) simulations are advantageous in revealing atomic-scale structure evolution and in interpreting the relevant experiments at the microscopic level. Many of the simulations of the physical processes which have similarities with explosive welding process, such as diffusion bonding, were carried out by MD simulations. Chen *et al.*[11] used MD simulations to investigate the effects of temperature and surface roughness on diffusion bonding in a Cu-Al system, whereas the simulations were quasi-static and there were no collisions. Delogu[12] studied the collisions between two Ni crystals with surfaces at relative velocities in the range between 1 and 100 m/s, nevertheless, the impact velocities were not high enough. Zhao *et al.*[13] showed that shock-induced melting played a key role in accelerating the initiation and propagation of self-sustained exothermic alloying reactions in Ni/Al nanolaminates, however, the relative impact velocity was 4000 m/s which is much higher than the actual impact velocity of explosive welding, and the study did not involve diffusion.

In this study, we use MD simulations to shed light on atomic diffusion behavior in Cu-Al explosive welding process, and eventually propose a hybrid method based on classical diffusion theory to calculate the thickness of the diffusion layer. In addition, the diffusion features at the bonding interface are investigated in detail. In order to verify the method, a Cu-Al weldment is prepared by explosive welding technique, and the experimental result is compared with the corresponding numerical result.

II. METHODOLOGY

A. MD simulations

Our MD simulations are performed with the LAMMPS package.[14] For all simulations, a constant integration time step of 1 fs is used. The atom interactions are described by Cai and Ye's[15] embedded atom method alloy potential for Cu and Al. The simulation processes mainly contain two steps: the initialization and the collision. Fig. 1 presents the configuration of the initialization. Two separated metal bulks, Cu (21 000 atoms)

a)Author to whom correspondence should be addressed. Electronic mail: kliu@pku.edu.cn. Tel.: +86 10 62765844.

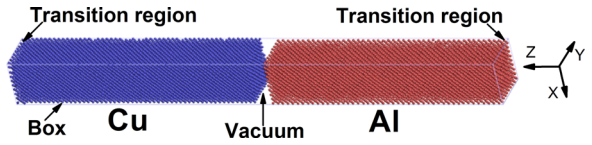

FIG. 1. The configuration of the initialization. The light blue wireframe represents the simulation box.

and Al (15 066 atoms), are put inside a simulation box with dimensions of $3.6(X) \times 3.6(Y) \times 39.6(Z)$ nm^3. The contact surfaces of Cu and Al are both (0 0 1) planes. Between them, vacuum is used to isolate the bulks' initial free surfaces. On both the nonimpact sides along the z axis, two transition regions which have 3 layers of atoms, respectively, are used to reduce the high speed shock waves' influence. Periodic boundary conditions are applied in the x, y directions. The initial thermal velocities of atoms are assumed to follow the Maxwellian distribution. With Nose-Hoover thermostat[16] adopted, the whole system is relaxed at 300 K and zero external pressure under the constant-pressure-temperature (NPT) ensemble to finish the initialization.

Then the Cu bulk is given a velocity to simulate the collision. The system is relaxed for 1000 ps under the microcanonical (NVE) ensemble. In the end, with the final equilibrium temperature of the NVE simulation kept, the system is relaxed for another 1000 ps at zero external pressure (NPT ensemble). In brief, the simulation of the collision is divided into two stages: the loading stage and the unloading stage. And this division method is consistent with the previous study focusing on explosive welding.[17] The collisions with and without transverse velocity are simulated, respectively. The former are simulated when u_z is set at every 250 m/s from 250 m/s to 2500 m/s. And the latter are simulated when u_z is set at 1500 m/s and u_x is set at every 100 m/s from 100 m/s to 900 m/s.

B. Explosive welding experiments

In order to verify the simulation results, relevant verification experiments are carried out. The basic facts about such a welding process can be found in Refs. 1–6.

Figure 2(a) presents the sketch of initial configuration for our explosive welding technique. As shown in Fig. 2(a), the steel chopping block with a thickness of 5 cm is placed at the bottom. An Al 1060 plate is laid on the chopping block as the base plate. Four supports stand on the Al 1060 plate and support a Cu T2 plate. Supports are put on the four corners of the Al plate, and they will fly off at the beginning of explosive welding. A special mixed explosive is spread on the Cu plate. The explosive is mixed with ammonium nitrate fuel oil mixture (AN explosive) and hexogen (5%–8%). Its actually measured detonation velocity can reach 3800–4100 m/s. An electric detonator is embedded in the left part of the explosive. By triggering the electric detonator, the explosive is detonated and drives the Cu plate to the Al plate. At the colliding point, the pressure and the temperature are so high that two materials join together. In the plate collision zone, the pressure impulse of about tens of GPa occurs. Fig. 2(b) presents the weldment obtained by the explosive welding technique from which we can find that the two materials join together very well. To inspect the diffusion layer thickness of the weldment, a specimen containing the bonding interface is subjected to scanning electron microscope (SEM, HITACHI S-4800) observation (see Fig. 2(c)). The bonding interface exhibits a straight morphology.

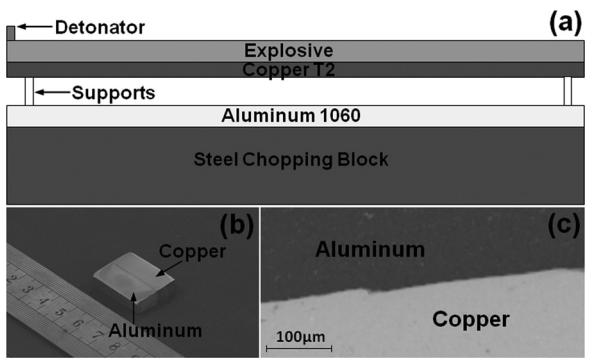

FIG. 2. (a) Sketch of the explosive welding technique. (b) Optical graph showing the Cu-Al weldment prepared by the explosive welding technique. (c) SEM micrograph of the interface which shows a straight morphology.

III. RESULTS AND DISCUSSION

A. MD simulations

Under the collision, the welding process can be divided into the loading stage and the unloading stage.[17] Fig. 3 presents the time history of the temperature and pressure of the whole system during the loading stage when $u_z = 1500$ m/s, $u_x = 700$ m/s. As shown in Fig. 3, with the system's kinetic energy changing into internal energy, the system temperature dramatically increases to about 1160 K in a time close to 45 ps. At the same time, the system pressure vibrates intensely. After about 300 ps, the temperature and the pressure maintain dynamic equilibrium at about 1160 K and 34 GPa, respectively. These phenomena are connected with overcoming the energy barrier and meeting atoms in a sufficiently short distance. The contact and activation allow the welding materials to generate the adhesion joint.

Fig. 4 presents the mean square displacement (MSD) curves when $u_z = 1500$ m/s, $u_x = 700$ m/s. In detail, Fig. 4(a) presents the MSD curves during the loading stage and Fig. 4(b) presents the MSD curves during the unloading stage. As shown in Fig. 4(a), the curves approximately parallel the

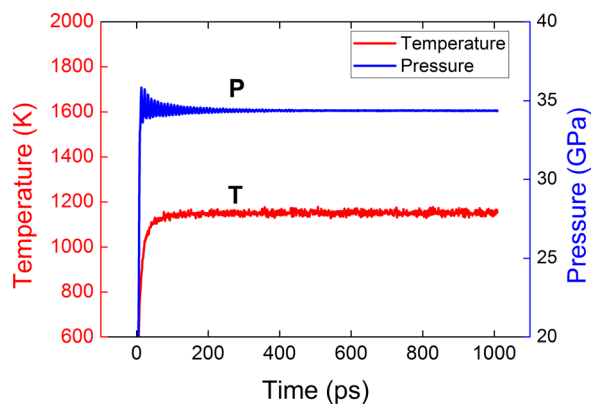

FIG. 3. The temperature and pressure curves of the whole system during the loading stage when $u_z = 1500$ m/s, $u_x = 700$ m/s.

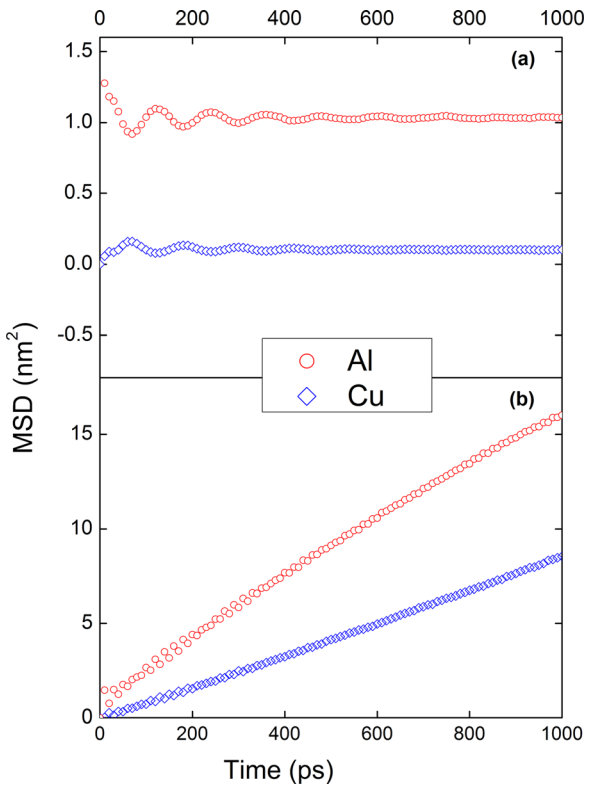

FIG. 4. MSD curves when $u_z = 1500$ m/s, $u_x = 700$ m/s. (a) The loading stage. (b) The unloading stage.

Time axis after some fluctuations. Finally, the MSD of Cu stabilizes at about 0.1 nm^2, while that of Al stabilizes at about 1.0 nm^2. It indicates that the whole system remains solid through the loading stage though the system temperature is more than the melting point under atmospheric pressure of Al. This is because the melting point of Al increases significantly as the pressure increases. No obvious diffusion takes place in the loading stage. Obvious diffusion mainly takes place in the unloading stage. As shown in Fig. 4(b), the MSD of Cu and Al keep increasing over time and reach about 8.5 nm^2 and 16.2 nm^2, respectively, after 1000 ps. The curves approximate straight lines. It demonstrates that the system melts rapidly as soon as the system pressure has been unloaded. At the same time, Cu and Al atoms begin to diffuse from both sides of the interface, and the diffusivity of Al is larger than that of Cu under the given velocity condition.

The atomic diffusion behavior under different speed conditions has different characteristics. Fig. 5 presents configurations of (1,0,0) planes under different transverse velocities at 200 ps after the unloading stage begins. When $u_x = 100$ m/s (Fig. 5(a)), there is no obvious diffusion on both sides. The Cu side retains its initial fcc lattice structure while the Al side exhibits an amorphous structure. When $u_x = 300$ m/s (Fig. 5(b)), several Cu atoms and a few Al atoms have diffused into their opposite side, and the diffusion depth of Cu is greater than that of Al. When u_x is higher than 300 m/s as shown in Figs. 5(c) and 5(d), more significant diffusion of both Cu atoms and Al atoms is seen, forming the diffusion layer. But the difference between the diffusion depths of Cu and Al gets smaller. When $u_x = 700$ m/s (Fig. 5(d)), the Cu

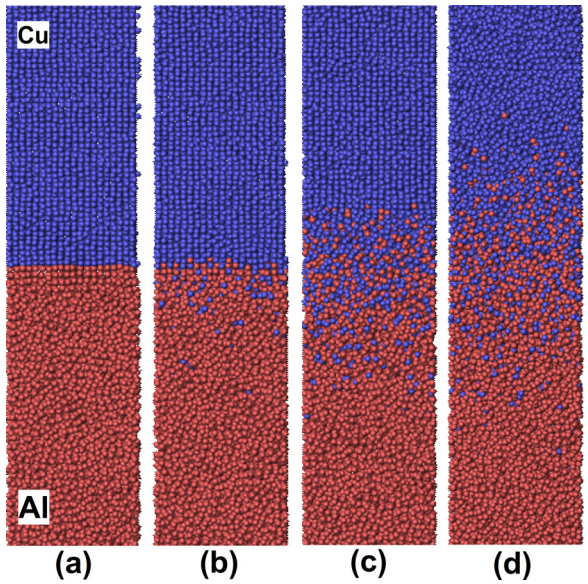

FIG. 5. Configurations of (1,0,0) planes when $u_z = 1500$ m/s, $u_x =$ (a) 100 m/s, (b) 300 m/s, (c) 500 m/s, (d) 700 m/s are obtained at 200 ps after the unloading stage begins. Only atoms near the interface are shown. Cu atoms are at the top and Al atoms are at the bottom.

side begins to exhibit an amorphous structure, and there is no apparent difference between the diffusion depths of Cu and Al. These phenomena should mainly result from that the melting point of Cu (1356 K) is much higher than that of Al (933 K). With the collision velocity increasing, the temperature of the system increases. When the temperature exceeds the melting point of Al but is still lower than that of Cu, the bonds in Al are broken and lots of vacancies form whereas the Cu side still keeps its lattice structure. So it is easy for Cu atoms to diffuse into the Al side whereas few Al atoms can diffuse into the Cu lattice. With the temperature further increasing, the bonds between Cu atoms become weaker and weaker, and the difference between the diffusion depths of Cu and Al gets smaller and smaller. When the temperature exceeds the melting point of Cu, the difference can hardly be distinguished only by means of observing the simulation images.

Moreover, as shown in Fig. 5, the higher the collision velocity is, the more intense the atoms diffuse. There is a certain correlation between the diffusion coefficient and the collision velocity. According to the Einstein diffusion law, the diffusion coefficient is presented as

$$D = \lim_{t\to\infty} \frac{1}{2\mathbb{N}t} \langle |\mathbf{r}(t) - \mathbf{r}(0)|^2 \rangle, \tag{1}$$

where $\mathbb{N}$ is the dimensionality of the system. Here, we consider the simulation configuration as unidimensional and take $\mathbb{N} = 1$, so that half of the slopes of the MSD curves are the diffusion coefficients. MSD curves during the unloading stage at all the given velocities are obtained. The curves at low velocities are similar to the curve during the loading stage which is shown in Fig. 4(a), and these curves are not considered any more. The curves similar to the curves shown in Fig. 4(b) are linear fitted and the corresponding diffusion coefficients are calculated.

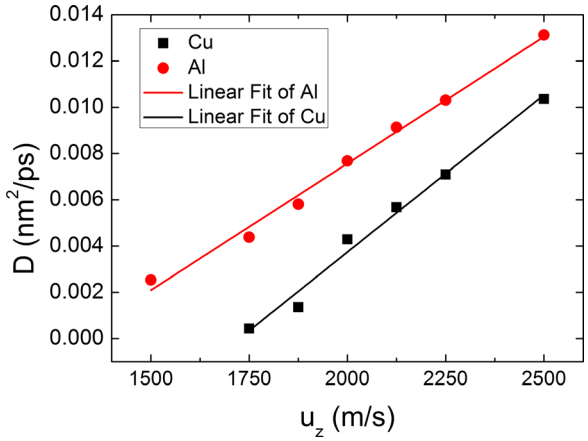

FIG. 6. Diffusion coefficients of Cu and Al at different longitudinal velocities. The straight lines are the results of the linear fit.

Fig. 6 presents the relation between the diffusion coefficients of Cu and Al and the longitudinal velocity. The two straight lines are the results of the linear fit. As shown in Fig. 6, without transverse velocity, Al atoms diffuse obviously when u_z exceeds 1500 m/s, while Cu atoms diffuse obviously when u_z exceeds 1750 m/s. The diffusion coefficient of Al is larger than that of Cu at the same longitudinal velocity. The diffusion coefficient is directly proportional to the longitudinal velocity.

Fig. 7 presents the relation between the diffusion coefficients of Cu and Al and the transverse velocity, when the longitudinal velocity is fixed at 1500 m/s. The transverse velocities are set at every 100 m/s from 100 m/s to 900 m/s. The results are treated with a quadratic fit processing. As shown in Fig. 7, Al atoms diffuse obviously when u_x is above 100 m/s, while Cu atoms diffuse obviously when u_x is above 300 m/s. The diffusion coefficient of Al is larger than that of Cu at the same transverse velocity. The diffusion coefficient is directly proportional to the square of the transverse velocity. Comparing Fig. 7 with Fig. 6, we can see that the influence of transverse velocity on the diffusion coefficient is one order higher than that of longitudinal velocity. This should be one of the reasons why the explosive welding techniques adopt skew collision. The transverse velocity helps induce

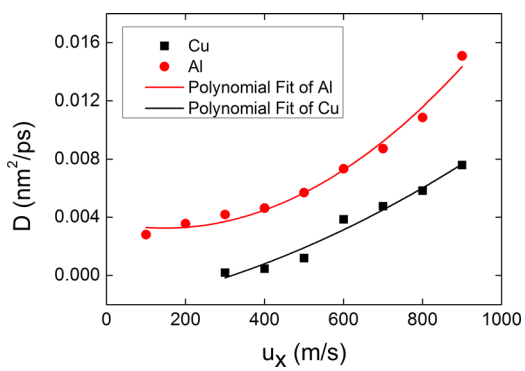

FIG. 7. Diffusion coefficients of Cu and Al at different transverse velocities with the longitudinal velocity fixed at 1500 m/s. The transverse velocities are adopted at every 100 m/s from 100 m/s to 900 m/s. The curves are the results of the polynomial fit whose order is 2.

shear deformation. Numerous experiments have shown that physical processes accelerate more abruptly if the compression is accompanied by shear deformation. This point of view was first suggested in Ref. 18 and discussed in Refs. 19 and 20. In addition, the shear deformation also helps result in breakup of a crystal lattice, and then the diffusion activation energy could decrease to a value corresponding to a liquid or even to a smaller magnitude.

In order to get deeper understanding of the diffusion in Cu-Al explosive welding process, we try to calculate the thickness of the diffusion layer by means of a hybrid method. Under isothermal condition, when the system achieves equilibrium, the regular diffusion process of Cu and Al should meet the classical diffusion equation which can be expressed as

$$\partial n/\partial t = D\nabla^2 n, \tag{2}$$

where n is the atom concentration, t is the diffusion time, and D is the diffusion coefficient. One of its conventional solutions is

$$n(x,t) = \frac{N}{2\sqrt{\pi Dt}}\exp(-x^2/4Dt), \tag{3}$$

where N is the quantity of the diffusion matter, and x is the diffusion distance. Obviously, it is a Gaussian distribution function, and we have

$$\int_0^{3\sqrt{2Dt}} n(x,t)dx/N \approx 99.7\%. \tag{4}$$

Thus, we can calculate the thickness of the diffusion layer L by

$$L = \sum_{i=Cu,Al} 3\sqrt{2D_i t}. \tag{5}$$

Yan *et al.*[21] showed that the unloading stage in the explosive welding practice could last for 5–10 μs. Due to constraints on the time scale, MD simulations cannot capture the evolution of the system for so long time. However, Yan *et al.* also showed that the decrease in the system temperature is small during the unloading stage, so we can treat the unloading stage as isothermal. The classical diffusion theory demonstrates that the diffusion coefficient keeps invariable under isothermal condition. So, though our MD simulations for the unloading stage only last for 1000 ps, we have good reasons to extrapolate the duration of the diffusion to 5–10 μs with a constant diffusion coefficient.

To verify the accuracy of Eq. (5), a simulation test is done first. Take the case $u_z = 1500$ m/s, $u_x = 600$ m/s as example, the thicknesses of the diffusion layer at every 100 ps in the unloading stage are calculated by Eq. (5). By extracting the coordinate information of the atoms from the LAMMPS dump files, the thicknesses of the diffusion layer can also be obtained. The two kinds of results are compared and shown in Fig. 8. The two kinds of results have similar values and the same trend within the actual simulation time. Similar

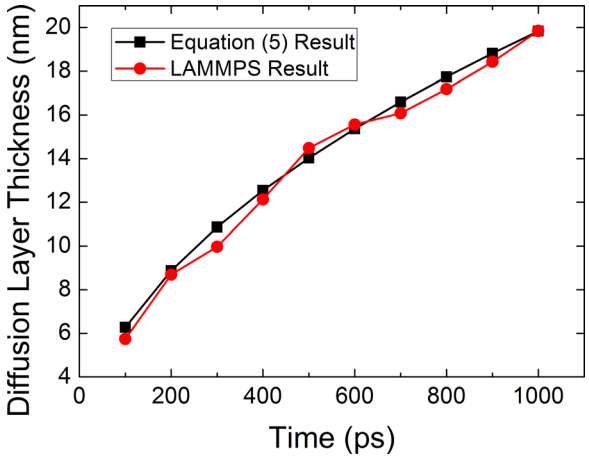

FIG. 8. Results about the thicknesses of the diffusion layer at every 100 ps obtained by Eq. (5) and the LAMMPS simulations, respectively.

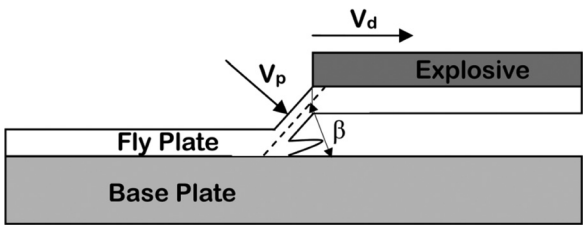

FIG. 9. The schematic view of the explosive welding process in our verification experiment. V_p is the flyer plate velocity, V_d is the detonation velocity, and β is the flyer plate dynamic bend angle.

test results are also obtained under other velocity conditions. So the validity of Eq. (5) is preliminarily confirmed and it paves the way for further verification experiments.

B. Verification experiments

Fig. 9 shows the schematic view of the explosive welding process in our verification experiment. The following equation[6] holds for the parallel gap geometry illustrated in Fig. 9:

$$V_p = 2V_d \sin(\beta/2), \tag{6}$$

where V_p is the flyer plate velocity, V_d is the detonation velocity, and β is the flyer plate dynamic bend angle. As previously mentioned, V_d in our experiment is from 3800 m/s to 4100 m/s. According to Eq. (6), V_p at a given transverse velocity can be obtained and it is in a range (see Table I). The flyer plate velocity adopted in the simulation is denoted by V'_p and we have

TABLE I. Corresponding results calculated by Eq. (6) at some transverse velocities when the longitudinal velocity u_z is 1500 m/s.

u_x (m/s)	β	$\sin(\beta/2)$	V_p (m/s) ($V_d = 3800$ m/s)	V_p (m/s) ($V_d = 4100$ m/s)	$V'_p = \sqrt{u_x^2 + u_z^2}$ (m/s)
600	21.8°	0.189	1436	1550	1616
700	25°	0.216	1642	1771	1649
800	28.1°	0.243	1847	1993	1700

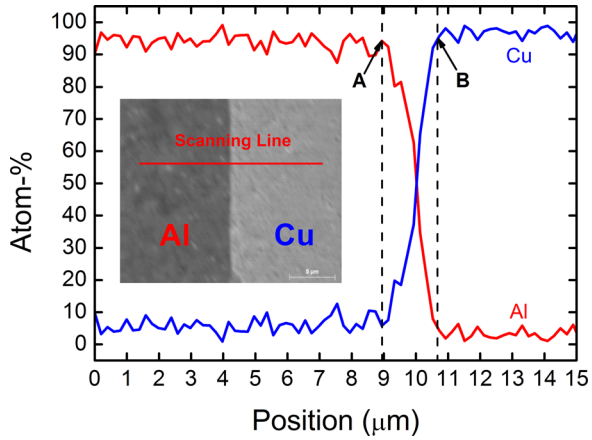

FIG. 10. SEM image of element counts by line-scan of X-ray photoelectron spectroscopy analysis aimed at some local area at the bonding interface. The curves represent the percentage of the atom number at positions along the scanning line. The dashed lines indicate the diffusion region. Point A and point B are points of intersection of the dashed lines and the curves, respectively. The magnification of the inner image is 10 000.

$$V'_p = \sqrt{u_x{}^2 + u_z{}^2}. \tag{7}$$

V'_p should be in the range of the corresponding V_p. The simulation whose $u_x = 700$ m/s is the only one that meets the requirement (see Table I), i.e., the velocity adopted in this simulation is the closest to our experiment. Using the diffusion coefficients of this simulation, we attain that the diffusion layer thickness is in a range from 1.54 μm (the corresponding diffusion time is 5 μs) to 2.18 μm (the corresponding diffusion time is10 μs).

Fig. 10 presents one of the three results of component analysis by EDS line scanning. The curves represent the percentage of the atom number at positions along the scanning line. The percentages of the atom number at point A and point B are both 95%. In accordance with this standard, the width of the region between the dashed lines represents the thickness of the diffusion layer, and it is 1.79 μm. The other two EDS results are 1.98 μm and 2.18 μm, respectively. So the average of the three is 1.98 μm. The simulation results and the experimental results fit very well.

IV. CONCLUSIONS

The diffusivities in the loading stage and the unloading stage are quite distinct from each other. Diffusion mainly takes place in the unloading stage. The diffusivities of Cu atoms and Al atoms are also quite different under different collision velocity conditions. As a result of the difference between the welding points of Cu and Al, Cu atoms diffuse more easily into the Al side under relatively low collision velocity, while Al atoms diffuse more intense under relatively high collision velocity. When there is no transverse velocity, the diffusion coefficient is directly proportional to the longitudinal velocity. With the longitudinal velocity fixed, the diffusion coefficient is proportional to the square of the transverse velocity. The influence of transverse velocity on the diffusion coefficient is one order higher than that of longitudinal velocity. Although skew collision has been widely adopted in explosive welding industry for decades, the

mechanism has not been very clear. Our study reveals the mechanism from the perspective of diffusion at the atomic scale. This can provide ideas for improvement of the welding quality, such as the precise design for the collision angle. Our hybrid method for calculating the thickness of diffusion layer is combined with the classical theory and MD simulations. The feasibility of the method is confirmed by simulation tests and verification experiments.

ACKNOWLEDGMENTS

This work has been supported by the National Natural Science Foundation of China (Grant Nos. 10732010, 10972010, 11028206, and 2012M510270) and Tan Chin Tuan exchange fellowship in engineering.

[1]F. Grignon, D. Benson, K. S. Vecchio, and M. A. Meyers, Int. J. Impact Eng. **30**, 1333 (2004).
[2]M. Acarer, B. Gulenc, and F. Findik, Mater. Des. **24**, 659 (2003).
[3]M. Acarer and B. Demir, Mater. Lett. **62**, 4158 (2008).
[4]J. Z. Ashani and S. M. Bagheri, Materialwiss. Werkstofftech. **40**, 690 (2009).
[5]K. X. Liu, W. D. Liu, J. T. Wang, H. H. Yan, X. J. Li, Y. J. Huang, X. S. Wei, and J. Shen, Appl. Phys. Lett. **93**, 081918 (2008).
[6]F. Findik, Mater. Des. **32**, 1081 (2011).
[7]P. V. Vaidyanathan and A. Ramanathan, J. Mater. Process. Technol. **38**, 501 (1993).
[8]A. Abe, J. Mater. Process. Technol. **85**, 162 (1999).
[9]S. A. A. Akbari Mousavi and P. F. Sartangi, Mater. Sci. Eng., A **494**, 329 (2008).
[10]K. Hokamoto, K. Nakata, A. Mori, S. Ii, R. Tomoshige, S. Tsuda, T. Tsumura, and A. Inoue, J. Alloys Compd. **485**, 817 (2009).
[11]S. Chen, F. Ke, M. Zhou, and Y. Bai, Acta Mater. **55**, 3169 (2007).
[12]F. Delogu, Phys. Rev. B **82**, 205415 (2010).
[13]S. Zhao, T. Germann, and A. Strachan, Phys. Rev. B **76**, 104105 (2007).
[14]S. Plimpton, J. Comput. Phys. **117**, 1 (1995).
[15]J. Cai and Y. Y. Ye, Phys. Rev. B **54**, 8398 (1996).
[16]D. J. Evans and B. L. Holian, J. Chem. Phys. **83**, 4069 (1985).
[17]B. Wronka, J. Mater. Sci. **45**, 3465 (2010).
[18]B. J. Alder, *Solids under pressure* (McGraw-Hill, New York, 1963).
[19]A. N. Dremin and O. N. Breusov, Russ. Chem. Rev. **37**, 392 (1968).
[20]L. S. Vasil'ev, Phys. Met. Metallogr. **107**, 427 (2009).
[21]H. Yan, Y. Qu, and X. Li, Combust., Explos. Shock Waves **44**, 491 (2008).